ELSEVIER

Journal of Biomechanics 32 (1999) 531–537

JOURNAL OF BIOMECHANICS

Technical Note

Constitutive model of brain tissue suitable for finite element analysis of surgical procedures

Karol Miller*

Department of Mechanical and Materials Engineering, The University of Western Australia, Nedlands/Perth WA 6907, Australia

Received in final form 20 December 1998

Abstract

Realistic finite element modelling and simulation of neurosurgical procedures present a formidable challenge. Appropriate, finite deformation, constitutive model of brain tissue is a prerequisite for such development. In this paper, a large deformation, linear, viscoelastic model, suitable for direct use with commercially available finite element software packages such as ABAQUS is constructed. The proposed constitutive equation is of polynomial form with time-dependent coefficients. The model requires four material constants to be identified. The material constants were evaluated based on unconfined compression experiment results. The analytical as well as numerical solutions to the unconfined compression problem are presented. The agreement between the proposed theoretical model and the experiment is good for compression levels reaching 30% and for loading velocities varying over five orders of magnitude. The numerical solution using the finite element method matched the analytical solution very closely.

Keywords: Brain tissue; Mechanical properties; Mathematical modelling; Finite element method

1. Introduction

The investigation into the mechanical properties of 'very' soft tissues, which do not bear mechanical loads (such as brain, liver, kidney, etc.), has not been in the centre of scientific effort. In recent years, however, we have witnessed a rapid advance in various robotics technologies relevant to medical applications. New automatic surgical tools and robots (e.g. Brett et al., 1995) as well as virtual reality techniques (e.g. Burdea, 1996) have been developed, creating a need for accurate soft tissue and organ models. Such mathematical models of 'very' soft tissue mechanical properties may find applications, for example, in a surgical robot control system, (Miller and Chinzei, 1995a, b), surgical operation planning and surgeon training systems based on the virtual reality techniques (Burdea, 1996 and references cited therein), and *registration* (Lavallée, 1995).

The reported experimental data on the mechanical properties of brain tissue under large deformation conditions are limited almost exclusively to compressive loading (see Miller and Chinzei, 1997 and references cited therein). Miller and Chinzei (1997) conducted compressive tests on swine brain tissue and proposed non-linear viscoelastic model describing tissue behaviour in compression for strains up to 30% and strain rates between 0.64×10^{-5} to 0.64 1/s. Recently, Guillaume et al. (1997) discussed brain response to hypergravity, and Donnelly and Medige (1997) investigated human brain tissue properties in shear. However, very high strain rates applied in those studies prohibit the use of results for modelling surgical procedures.

In this paper we develop a finite deformation, linear viscoelastic model of brain tissue. The proposed model is shown to describe well brain tissue deformation behaviour under compression, at low strain rates, typical for neurosurgical procedures. The proposed model can be immediately used with ABAQUS finite element analysis software.

2. Constitutive modelling of brain tissue

2.1. Brain as a viscoelastic single-phase continuum

Recently brain tissue constitutive models based on the strain energy function in polynomial form with time-dependent coefficients have been proposed (Mendis et al.,

* Fax: + 61 89380 1024; e-mail: kmiller@mech.uwa.edu.au

0021-9290/99/$ – see front matter
PII: S0021-9290(99)00010-X

1995; Miller and Chinzei, 1997). The applicability of the model by Mendis is restricted to very high strain-rate loading conditions, typical for injury modelling. The model by Miller and Chinzei is suitable for low strain-rates typical for surgical procedures. However, it is non-linearly viscoelastic. This causes problems in its finite element implementation.

For the details of the hyperelastic, linear viscoelastic constitutive model see ABAQUS Manual (ABAQUS, 1994) and references cited therein. Here we note only that the polynomial strain energy function of the hyperelastic, linear viscoelastic medium can be written in the following form:

$$W = \int_0^t \left\{ \sum_{i+j=1}^{N} \left[C_{ij0} \left(1 - \sum_{k=1}^{n} g_k (1 - \mathrm{e}^{-(t-\tau)/\tau_k}) \right) \right] \times \frac{\mathrm{d}}{\mathrm{d}\tau} [(J_1 - 3)^i (J_2 - 3)^j] \right\} \mathrm{d}\tau, \quad (1)$$

where τ_k are characteristic times, g_k are relaxation coefficients, N is the order of polynomial in strain invariants (as a result of the assumption of the brain tissue initial isotropy the energy depends on the histories of strain invariants only) used for strain energy function description and J_1, J_2, J_3 are strain invariants:

$$J_1 = \mathrm{Trace}[\mathbf{B}], \quad J_2 = \frac{J_1^2 - \mathrm{Trace}[\mathbf{B^2}]}{2J_3},$$

$$J_3 = \sqrt{\det \mathbf{B}} = 1. \quad (2)$$

B is a left Cauchy–Green strain tensor. The common assumption of tissue incompressibility results in the third strain invariant being equal to one.

Parameters C_{ij0} describe the instantaneous elasticity of the tissue. For infinitesimal strain conditions, the sum of constants C_{100} and C_{010} has a physical meaning of one half of the instantaneous shear modulus, i.e.:

$$\frac{\mu_0}{2} = C_{100} + C_{010}. \quad (3)$$

The application of such linear viscoelastic model requires the estimation of constants C_{ij0} describing the instantaneous behaviour of the tissue as well as g_k and τ_k, $k = 1, \ldots, n$ governing the time-dependent tissue behaviour.

2.2. Determination of material constants for swine brain tissue

For the determination of material coefficients for the model, the experimental results for the loading phase of the unconfined compression of swine brain tissue for the following three loading velocities (Miller and Chinzei, 1997) were used:

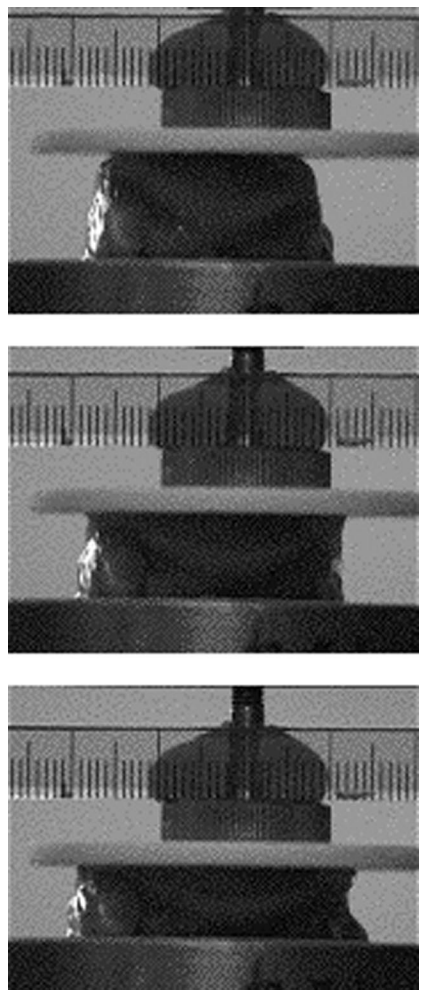

Fig. 1. Approximately uniform expansion of a brain specimen undergoing unconfined compression as captured by a CCD camera.

Fast: 500 mm min^{-1}, corresponding to the strain rate of about 0.64 s^{-1} (12 samples),
Medium: 5 mm min^{-1}, corresponding to the strain rate of about 0.64×10^{-2} s^{-1} (13 samples), and
Slow: 0.005 mm min^{-1}, corresponding to the strain rate of about 0.64×10^{-5} s^{-1} (six samples).

Eight swine brains were used for the experiments. The stress–strain curves were concave upward for all compression rates containing no linear portion from which a meaningful elastic modulus could be determined. The tissue response stiffened with the increasing loading speed, indicating a strong stress–strain rate dependence.

When conducting the experiments care was taken to diminish friction between platens and a specimen. As a result samples under compression expanded uniformly, Fig. 1. Therefore, it is assumed that under unconfined compression experiment conditions the deformation was orthogonal, and hence the left Cauchy–Green strain

tensor had only diagonal components:

$$\mathbf{B} = \begin{bmatrix} \lambda_z^2 & 0 & 0 \\ 0 & \lambda_z^{-1} & 0 \\ 0 & 0 & \lambda_z^{-1} \end{bmatrix}, \tag{4}$$

where λ_z is a stretch in vertical direction. Taking $J_1 = \lambda_z^2 + 2\lambda_z^{-1}$ and $J_2 = \lambda_z^{-2} + 2\lambda_z$, the only non-zero Lagrange stress components can be computed from the simple formula:

$$T_{zz} = \frac{\partial W}{\partial \lambda_z}. \tag{5}$$

Upon substitution of (1) into (5) one obtains:

$$T_{zz} = \int_0^t \left\{ \sum_{i+j=1}^{N} \left[C_{ij0}\left(1 - \sum_{k=1}^{n} g_k\left(1 - \mathrm{e}^{-(t-\tau)/\tau_k}\right)\right)\right] \times \frac{\mathrm{d}}{\mathrm{d}\tau}\left[\frac{\partial}{\partial \lambda_z}\left((J_1 - 3)^i (J_2 - 3)^j\right)\right]\right\} \mathrm{d}\tau. \tag{6}$$

To obtain a good agreement between the theory and experiment, it was necessary to retain second-order terms in energy function (1). Then, for $N = 2$:

$$\begin{aligned} T_{zz} = \int_0^t \left\{ \left(1 - \sum_{k=1}^{n} g_k\left(1 - \mathrm{e}^{-(t-\tau)/\tau_k}\right)\right) * \left[C_{100}\frac{\mathrm{d}}{\mathrm{d}\tau}(2\lambda_z - 2\lambda_z^{-2}) \right.\right. \\ + C_{010}\frac{\mathrm{d}}{\mathrm{d}\tau}(-2\lambda_z^{-3}) + C_{110}\frac{\mathrm{d}}{\mathrm{d}\tau}[(\lambda_z^2 + 2\lambda_z^{-1} - 3) \\ \times (\lambda_z^{-2} + 2\lambda_z - 3)] \\ + C_{200}\frac{\mathrm{d}}{\mathrm{d}\tau}[(\lambda_z^2 + 2\lambda_z^{-1} - 3)(2\lambda_z - 2\lambda_z^{-2})] \\ \left.\left. + C_{020}\frac{\mathrm{d}}{\mathrm{d}\tau}[(\lambda_z^{-2} + 2\lambda_z - 3)(-2\lambda_z^{-3})] \right] \right\} \mathrm{d}\tau. \end{aligned} \tag{7}$$

In the case of the compression with constant velocity, integral (7) can be evaluated analytically (see the appendix). It is important to note here, that after fixing the values of parameters g_k the expression for stress is linear in material parameters C_{ij0}. Similarly, after fixing constants C_{ij0} the model becomes linear in parameters g_k. This important property was used in the procedure to estimate the values of material constants for swine brain tissue.

Two time-dependent terms ($n = 2$ in Eq. (7)) were used. This was a minimal number of exponentially decaying terms allowing for accurate modelling the tissue behaviour for a wide range of loading velocities. It proved not possible with only one exponentially decaying time-dependent term to reproduce the experimental results for strain rates ranging over five orders of magnitude. To uniquely determine material coefficients C_{ij0} and g_k (Eq. (7)) a few additional assumptions were adopted (Miller and Chinzei, 1997). The equality of the energy of reciprocal deformation to that of the original one (see Mooney, 1940) was assumed: $C_{010}/C_{100} = 1$ and $C_{020}/C_{200} = 1$. C_{110} was assumed to be equal 0. Two time constants, $\tau_1 = 0.5$ [s]; $\tau_2 = 50$[s], were chosen to be approximately equal to the duration of the medium and fast tests respectively. These assumptions left four constants to be determined: C_{100}, C_{200}, g_1 and g_2.

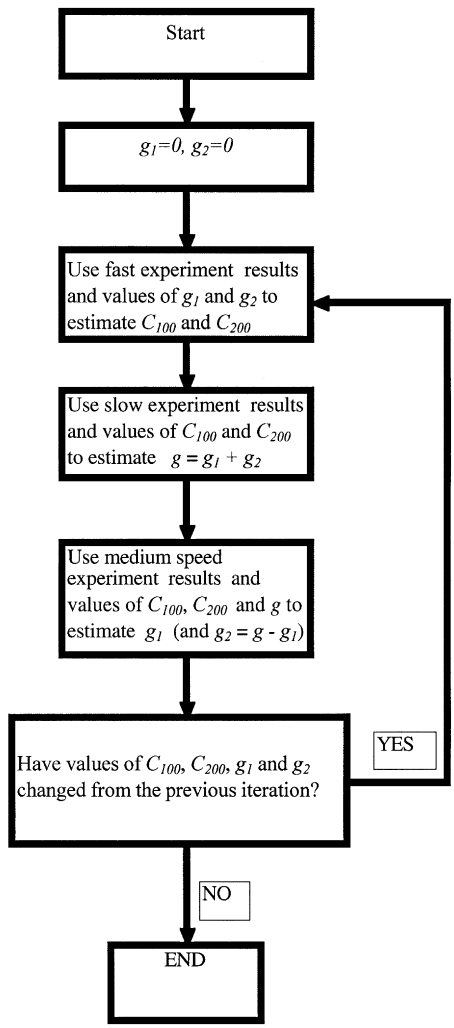

Fig. 2. Iterative procedure to determine constants C_{100}, C_{200}, g_1 and g_2.

A simple iterative procedure (Fig. 2) was used to uniquely determine the required four parameters. The strain rate of 0.64 1/s applied for the fast test in (Miller and Chinzei, 1997) is high for neurosurgical procedure standards. Therefore, it was initially assumed that the tissue behaviour for such strains is governed by parameters describing the instantaneous response: C_{100} and C_{200}. The influence of the parameters g_1 and g_2 on the results of the fastest test was initially assumed to be

negligible, so that, in the first iteration in the procedure of determining coefficients C_{100} *and* C_{200}, the remaining coefficients were set to zero. The function *Regress*, available in Mathematica software package (Wolfram Research, 1996), was used to find the least square fit to the fast test data. The values obtained were $C_{100} = 249$ Pa and $C_{200} = 427$ Pa.

Next, the results of the slow test were used to determine the value of $g = g_1 + g_2$. Characteristic times τ_1 and τ_2 are so small in comparison to the duration of the slow experiment that their influence can be neglected (this assumption was later confirmed by non-linear finite element simulation). Hence, for slow loading the expression for vertical stress reduces to

$$T_{zz} = -\frac{1}{\lambda_z^5}(2(-1+g1+g2)(-1-\lambda_z+\lambda_z^3+\lambda_z^4) \times (2C_{200} - 2C_{200}\lambda_z + C_{100}\lambda_z^2 - 2C_{200}\lambda_z^3 + 2C_{200}\lambda_z^4)) \quad (8)$$

and T_{zz} does not depend on g_1 and g_2 separately but on their sum g only. The Mathematica's function *Regress* was run again to find the least square estimate for g using slow test data. C_{100} and C_{200} were set as estimated from fast experiment results. The value obtained was $g = 0.798$.

Finally, the medium speed test results were used to estimate the value of g_1. In the first iteration function *Regress* provided $g_1 = 0.400$, and therefore $g_2 = g - g_1 = 0.398$. The estimated values of g_1 and g_2 were next used in the second iteration to estimate updated values of C_{100} and C_{200} from fast experiment results.

After repeating the procedure four times, the values of four coefficients sought converged. The estimated material properties of swine brain at low strain rates are listed in Table 1. Fig. 3 presents the comparison of experimental results and theoretical prediction of the linear viscoelastic model.

The agreement for fast and medium loading speeds is very good (Fig. 3 a, b). Worse match for slow loading speed results from a different character of the stress–strain curve than that for medium and fast loading speeds. This fact was taken into account in the non-linear model (Miller and Chinzei, 1997) by setting parameters $C_{20\infty}$ and $C_{02\infty}$ equal to zero and by suitable choice of C_{20k} and C_{02k}. Such flexibility is not possible in the linear model presented here. In the hyperelastic, linear viscoelastic model the shape of stress–strain curve does not depend on the strain rate (see Fig. 3).

2.3. Finite element simulation of unconfined compression experiment

To check the appropriateness of the proposed constitutive equation a finite element model of the unconfined compression experiment was constructed. The experiment was simulated using ABAQUS (1994) finite element analysis package.

Table 1
Brain material coefficients and multiple correlation coefficients

Instantaneous response	Characteristic time $t_1 = 0.5$ (s)	Characteristic time $t_2 = 50$ (s)
$C_{100} = C_{010} = 263$ (Pa); $C_{200} = C_{020} = 491$ (Pa); $R^2 = 0.996$	$g_1 = 0.450$; $R^2 = 0.986$	$g_2 = 0.365$; $R^2 = 0.986$

Four-hundred and eighty CAX4RH four-node, axisymmetric elements were used. Because of the tissue incompressibility the hybrid elements (with pressure as additional variable) were chosen. A boundary condition prescribing a velocity of a top layer of nodes was used to simulate indenter velocity. To simulate pure slip conditions a radial displacement was not fixed. Similarly at the bottom layer of nodes only the vertical displacements were constrained. Such a high number of elements enabled us to simulate other loading conditions as well.

ABAQUS command HYPERELASTIC was used to define instantaneous elasticity of the material (parameters C_{100} and C_{200}). Command VISCOELASTIC was used to model time-dependent tissue behaviour (parameters τ_1, τ_2, g_1 and g_2). To simulate the experimental conditions the procedure VISCO was applied. This procedure is best suited to simulating behaviour of hereditary viscoelastic materials. The time-dependent analyses were run for 0.72, 72 and 72,000 s for fast, medium and slow experiments, respectively. Time increments used were 0.01, 1 and 1000 s. After each time increment nodal values of the vertical component of the reaction forces on the top layer were summed and divided by the initial cross-section area, providing values of Lagrange stresses. The values of Lagrange stresses were used for comparison with the analytical solution given by Eq. (A.2), Fig. 3.

The numerical results match the analytical solution very closely, indicating the appropriateness of both analytical and numerical methods used. The very close agreement for slow loading conditions (Fig. 3c) indicates that the assumption of no influence of time-dependent terms on the analytical solution for slow loading (Eq. (8)) does not introduce an appreciable error.

3. Discussion and conclusions

In this study a simple, linear viscoelastic model of tissue deformation behaviour, suitable for direct finite element implementation is presented. The model accounts well for observed non-linear stress–strain

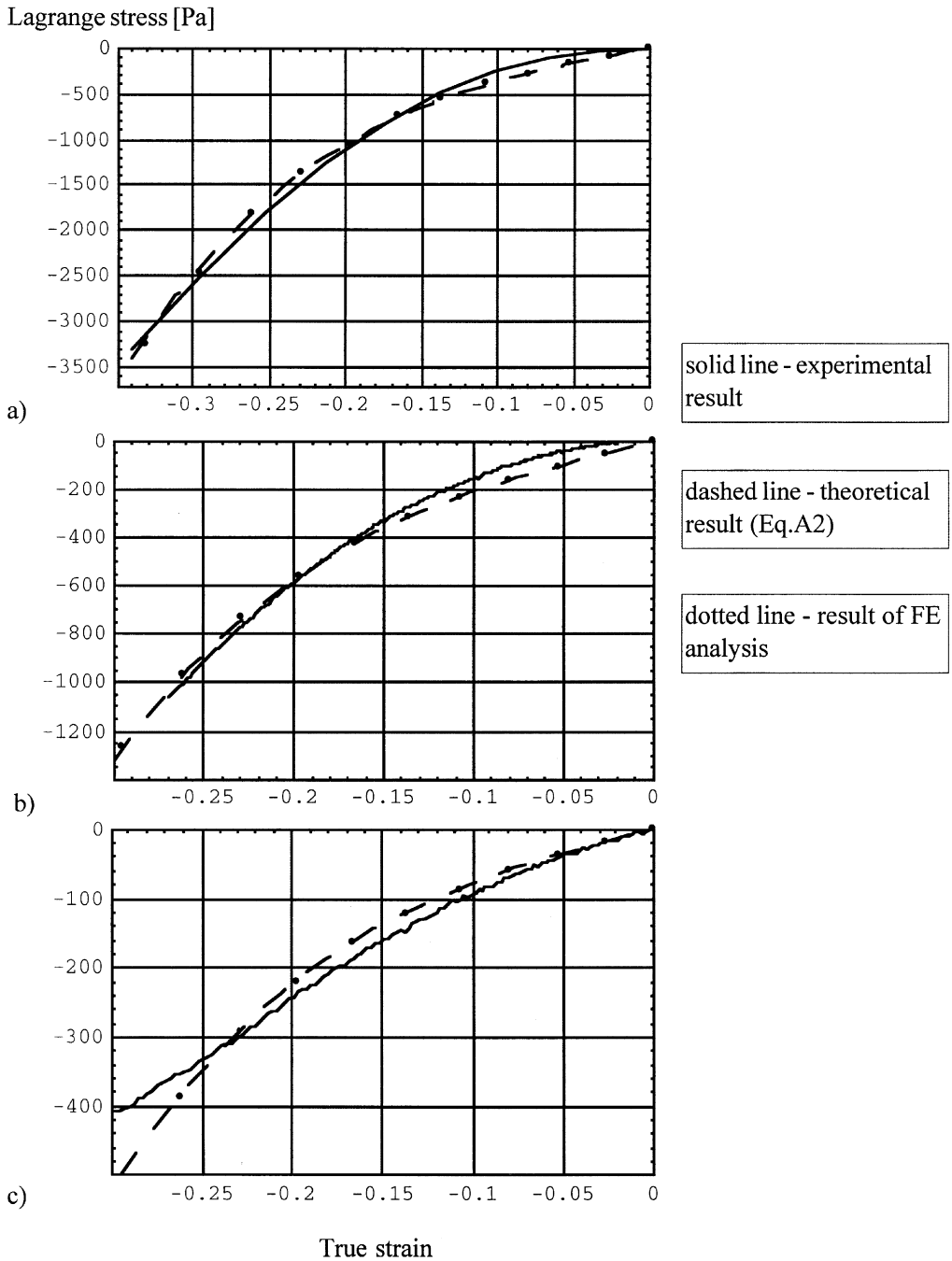

Fig. 3. Lagrange stress — true strain relations for swine brain tissue. Experimental, theoretical (analytical solution, Eq. (A.2)), and finite element analysis results (a) loading speed 500 mm/min, corresponding to the strain rate of about $0.64\,s^{-1}$, (b) loading speed 5 mm/min, corresponding to the strain rate of about $0.64 \times 10^{-2}\,s^{-1}$, (c) loading speed 0.005 mm/min, corresponding to the strain rate of about $0.64 \times 10^{-5}\,s^{-1}$.

relations, as well as for strong dependence between stresses and strain rate.

The use of the single-phase, linear, viscoelastic model based on the concept of the strain energy function, in the form of convolution integral with coefficient expressed in the form of exponential series, is described. The model developed here has a number of advantages over the previously proposed by this author, non-linear viscoelastic model (Miller and Chinzei, 1997). The new model requires only four material parameters to be identified — two fewer than in the non-linear model. The main advantage, though, is that the large deformation, linear viscoelastic model can be immediately applied to larger scale finite element computations by directly using

ABAQUS commands HYPERELASTIC — to describe instantaneous elasticity of the tissue, and VISCOELASTIC — to account for time dependent tissue behaviour.

Characteristic times used in this study are considerably larger than those used in hypergravity, impact and injury modelling. The tissue stiffness resulting from analysis of typical for surgical procedures, slow strain rate experiments, is much lower than that assumed in models intended to explain high strain rate phenomena. Therefore, one must be very cautious in choosing the appropriate model for one's anticipated strain rate range. The instantaneous stiffness governed by constants $C_{100} = 263$ Pa and $C_{200} = 491$ Pa will not, obviously, be adequate for describing tissue behaviour at strain rates larger than 0.7 1/s.

An alternative way of modelling brain tissue seems to be a biphasic approach. However, as it was shown in (Miller, 1998) biphasic models in their present form cannot account for strong stress–strain rate dependence observed in the brain tissue.

Acknowledgements

The financial support of Australian Research Council is gratefully acknowledged.

Appendix

The expression for the Lagrange stress can be divided into three parts: time independent – $T0$; time dependent, with characteristic time τ_1 – $T1$; and time dependent, with characteristic time τ_2 – $T2$. In case of unconfined compression with constant velocity the integral in Eq. (7) can be evaluated analytically. The result was obtained using Mathematica (Wolfram, 1996) software package:

$T0$ — see Eq. (*8*)

$$
\begin{aligned}
T1 = g1 \times & \left\{\frac{1}{v^3\tau_1^3}\left\{c_{100}\left\{E^{\lambda_z/(v\tau_1)}\,\mathrm{ExpIntegralEi}\left[-\frac{1}{v\tau_1}\right](1-2v\tau_1)\right.\right.\right. \\
& + E^{\lambda_z/(v\tau_1)}\,\mathrm{ExpIntegralEi}\left[-\frac{\lambda_z}{v\tau_1}\right](-1+2v\tau_1) \\
& + E^{(-1+\lambda_z)/(v\tau_1)}v\tau_1(1-3v\tau_1+4v^2\tau_1^2+2v^3\tau_1^3) \\
& - \frac{1}{\lambda_z^3}(v\tau_1(2v^2\tau_1^2+2v^3\lambda_z^3\tau_1^3 \\
& \left.\left.\left. + \lambda_z^2(1-2v\tau_1)+v\lambda_z\tau_1(-1+2v\tau_1))\right\}\right\}\right\} \\
& + \frac{1}{6v^5\tau_1^5}\left\{c_{200}\left\{E^{\lambda_z/(v\tau_1)}\,\mathrm{ExpIntegralEi}\left[-\frac{1}{v\tau_1}\right]\right.\right. \\
& \times(1-12v^2\tau_1^2+48v^3\tau_1^3) - E^{\lambda_z/(v\tau_1)} \\
& \times \mathrm{ExpIntegralEi}\left[-\frac{\lambda_z}{v\tau_1}\right](1-12v^2\tau_1^2+48v^3\tau_1^3) \\
& + E^{(-1+\lambda_z)/(v\tau_1)}v\tau_1(1-v\tau_1-10v^2\tau_1^2+54v^3\tau_1^3 \\
& - 48v^4\tau_1^4+48v^5\tau_1^5+144v^6\tau_1^6+144v^7\tau_1^7) \\
& - \frac{1}{\lambda_z^5}(v\tau_1(-6v^3\lambda_z\tau_1^3+24v^4\tau_1^4+72v^5\lambda_z^7\tau_1^5 \\
& + 144v^6\lambda_z^6\tau_1^6+24v^5\lambda_z^5\tau_1^5(-1+6v^2\tau_1^2) \\
& + \lambda_z^4(1-12v^2\tau_1^2+48v^3\tau_1^3) \\
& + \lambda_z^2(2v^2\tau_1^2-24v^4\tau_1^4) \\
& \left.\left.\left. - \lambda_z^3(v\tau_1-12v^3\tau_1^3+48v^4\tau_1^4))))\right\}\right\}, \qquad \text{(A.1)}
\end{aligned}
$$

where v is a loading velocity divided by specimen's initial hight. ExpIntegralEi denotes exponential integral function.

$T2$ is of identical form as $T1$. Characteristic time τ_1 should be replaced by τ_2 and g_1 by g_2.

$$T_{zz} = T0 + T1 + T2. \qquad \text{(A.2)}$$

References

ABAQUS Users Manual, 1994. Version 5.4, Hibbit, Karlsson & Sorensen, Inc.

Brett, P.N., Fraser, C.A., Henningan, M., Griffiths, M.V., Kamel, Y., 1995. Automatic surgical tools for penetrating flexible tissues. IEEE Engineering in Medicine and Biology 264–270.

Burdea, G., 1996. Force and Touch Feedback for Virtual Reality. Wiley, New York.

Donnelly, B.R., Medige, J., 1997. Shear properties of human brain tissue. Transactions ASME, Journal of Biomechanical Engineering 119, 423–432.

Guillaume, A., Osmont, D., Gaffie, D., Sarron, J.C., Quandieu, P., 1997. Effects of Perfusion on the mechanical behavior of the brain exposed to hypergravity. Journal of Biomechanics, 30(4), 383–389.

Lavallée, S., 1995. Registration for Computer Integrated Surgery: Methodology, State of the Art. Computer-Integrated Surgery. MIT Press, Cambridge, MA, pp. 77–97.

Mendis, K.K., Stalnaker, R.L., Advani S.H., 1995. A constitutive relationship for large deformation finite element modeling of brain tissue. Transactions ASME, Journal of Biomechanical Engineering 117, 279–285.

Miller, K., 1998. Modelling soft tissue using biphasic theory — a word of caution. Computer Methods in Biomechanics and Biomedical Engineering 1, 261–263.

Miller, K., Chinzei, K., 1995a. Modeling of soft tissues. Mechanical Engineering Laboratory News 12, 5–7 (in Japanese).

Miller, K., Chinzei, K., 1995b. Modeling of Soft Tissues Deformation, Journal Computer Aided Surgery, 1, (Suppl.) Proceedings of Second International Symposium on Computer Aided Surgery, Tokyo Women's Medical College, Shinjuku, Tokyo, pp. 62–63.

Miller, K., Chinzei K., 1997. Constitutive modelling of brain tissue; experiment and theory. Journal of Biomechanics 30(11/12), 1115–1121.

Mooney, M., 1940. A theory of large elastic deformation. Journal of Applied Physics 11, 582–592.

Wolfram, S., 1996. Mathematica Book, 3rd ed., Wolfram Media, Cambridge University Press, USA, pp. 816–820.

Wolfram Research, 1996. Mathematica 3.0 Standard Add-on Packages, Wolfram Media, Cambridge University Press, USA, pp. 428–439.